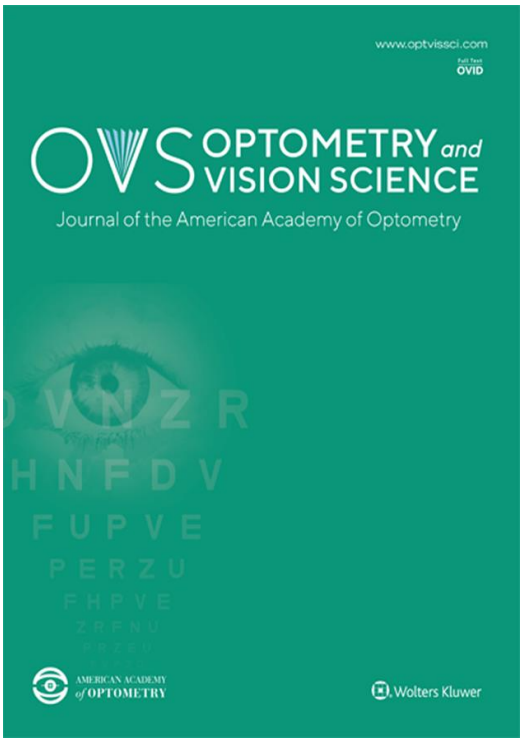

Optometry and Vision Science

Author's Accepted Manuscript

Article Title: Quantitative Assessment of Retinal and Choroidal Microvasculature in Asymptomatic Patients with Carotid Artery Stenosis

Authors: Monferrer-Adsuara C, Remolí-Sargues L, Navarro-Palop C, Cervera-Taulet E, Montero-Hernández J, Medina-Bessó P, Castro-Navarro V

DOI: 10.1097/OPX.0000000000002071

ORIGINAL INVESTIGATION

Quantitative Assessment of Retinal and Choroidal Microvasculature in Asymptomatic Patients with Carotid Artery Stenosis

Clara Monferrer-Adsuara, MD, Lidia Remolí-Sargues, MD, Catalina Navarro-Palop, MD, Enrique Cervera-Taulet, PhD, Javier Montero-Hernández, MD, Pascual Medina-Bessó, PhD, and Verónica Castro-Navarro, PhD

Hospital General Universitario de Valencia, Valencia, Spain (CM-A, LR-S, CN-P, EC-T, JM-H, VC-N), and Universidad de Valencia, Departamento de Fisiología Facultad de Medicina y Odontología, Valencia, Spain (PM-B)

Funding/Support: None of the authors have reported funding/support.

Conflict of Interest Disclosure: None of the authors have reported a financial conflict of interest.

Study Registration Information: -

Author Contributions: Conceptualization: CMA, LR-S, CN-P, EC-T, JM-H, PM-B, VC-N; Data Curation: CMA, LR-S, EC-T, JM-H, PM-B, VC-N; Formal Analysis: CMA, LR-S, PM-B, VC-N; Investigation: CMA, PM-B, VC-N; Methodology: CMA, PM-B, VC-N; Supervision: CN-P; Validation: CN-P; Writing – Original Draft: CMA; Writing – Review & Editing: CMA.

Submitted: February 10, 2023; accepted August 24, 2023.

Corresponding author:

Clara Monferrer-Adsuara

clara_cma@hotmail.com

ABSTRACT

Significance: Carotid disease contributes to 15–20% of all ischemic strokes, one of the leading causes of permanent disabilities and mortality globally. With its growing prevalence and the inflicted disability rates, screening for anomalies that precede the onset of its serious complications is of crucial global significance. **Purpose:** To assess the relationship between retinal and choroidal perfusion changes with the degree of stenosis using quantitative Swept-source optical coherence tomography angiography (SS-OCTA) in patients with internal carotid artery stenosis. **Methods:** A retrospective cohort study was conducted in 72 eyes with carotid stenosis. According to the degree of stenosis, the participants were divided into a healthy group (Group 1: 34 eyes), a mild-moderate stenosis group (Group 2: 22 eyes), a severe stenosis group (Group3: 16 eyes). SS-OCTA was performed to scan macular fovea. Capillary density values in the different retinal and choroidal layers were the major measurements for our study. **Results:** Mean vessel density in the mid-choroid layer was significantly higher in group 2 and 3 compared with group 1. Deep choroid disclosed significantly superior vascular density values in group 3 compared to groups 2 and 1. Superficial and deep capillary plexus showed decreased vascular density values when comparing group 3 with groups 1 and 2, although they were not significant. **Conclusions:** Our report provides the first evidence that choroidal microvascular changes were correlated with severity of carotid artery stenosis. OCTA can sensitively detect subtle, early changes in the ocular blood in carotid disease representing a useful, non-invasive and objective approach to the retinal microvasculature.

Carotid artery stenosis is a complex condition and a major risk factor for cerebral microcirculation dysfunction, being responsible for a wide spectrum of neurological disturbances such as transient ischemic attack, ischemic stroke, and vascular dementia.[1] Carotid artery stenosis contributes to 15–20% of all ischemic strokes,[2] one of the leading causes of permanent disabilities and mortality globally.[3] The prevalence of carotid artery stenosis rises with age, thus it is well recognized that about 5–10% of all patients aged 70 years or older suffer from carotid stenosis with ≥50% luminal narrowing, and a total of 10–15% of all novel strokes are secondary to untreated carotid stenosis.[4,5] With the growing prevalence of carotid stenosis, the great carotid artery stenosis -inflicted disability rates and the high economic weight imposed upon society, screening for anomalies that precede the onset of these serious complications is of crucial global significance, particularly for neurologically asymptomatic individuals.

Recently, substantial efforts have been made to develop affordable, noninvasive predictors of carotid artery stenosis. In actual guidelines, the degree of stenosis is a strong surrogate measurement for stroke risk and indication for treatment.[6] As the retina shares embryologic origin and microvascular features with the central nervous system,[7] retinal microvasculature has been hypothesized as a window into the state of brain circulation. Moreover, some published data indicates that anomalous retinal microvascular findings may act as biomarkers reflecting the severity of underlying cardiovascular and neurodegenerative microvascular conditions.[8,9] Since retinal blood flow is principally provisioned by the internal carotid artery, the authors speculate that structural alterations in the internal carotid artery may disturb the microcirculation and structure of the retina becoming biomarkers capable of identifying carotid stenosis subgroups especially prone to developing complications that could profit from early intervention.

The early anomalies of retinal vasculature associated with carotid artery stenosis have not been yet well determined partly because fundus images are not able to display a detailed retinal microvascular network. Conventional angiography may detect early changes but is an invasive technique. On the contrary, swept-source optical coherence tomography angiography (SS-OCTA) is a novel, in vivo imaging tool, that provides noninvasive, high-resolution assessment of the retinal vasculature without the use of intravenous dye. This technique also allows quantitative evaluation of the retinal and choroidal vessel density and subtle changes can be detected with high accuracy.[10]

Compared to spectral-domain OCTA, SS-OCTA presents a longer wavelength and a faster scan speed producing a more precise three-dimensional picture of the retinal microvasculature.[11] Triton SS-OCTA (DRI OCT Triton plus, Topcon, Tokyo, Japan) operates at a 1050 nm wave-length that enables improved penetration into tissue with a A-scan rate of 100 000 per second and uses an innovative OCTA algorithm, OCTARA (OCTA Ratio Analysis), that aims to provide improved detection sensitivity to low blood flow and reduced motion artifacts. [10] Thus, OCTARA can visualize the superficial retinal capillaries and foveal avascular zona, inner and outer retinal vascular plexuses, choriocapillaris, and larger choroidal vasculature in vivo without the need for contrast injection.

Currently, OCTA clinical utility is largely restricted to qualitative assessment of its grayscale images, but there have been recent efforts in quantitatively review the retinal and choriocapillaris vasculature in retinal diseases to aid in objective evaluation of the anomalies. The approaches of most of the studies have been the custom analysis on exported images, typically using the

publica domain ImageJ software (National Institutes of Health, Bethesda, MD), while only a few have employed the automated algorithms for mapping capillary density that some commercial OCTA manufacturers are including in their software.

There is a paucity of published data regarding the use of OCTA in a carotid artery stenosis clinical setting. Therefore, the aim of the current study is to assess the relationship between retinal and choroidal perfusion changes with the degree of stenosis, as measured using Triton SS-OCTA innovative algorithm OCTARA in patients with internal carotid artery stenosis.

METHODS

Study Design and Participants

This prospective non-randomized observational study adhered to the tenets of the Declaration of Helsinki and was approved by the institutional review board of the Consorcio Hospital General Universitario de Valencia where took place. All participants gave their written informed consent.

From June 2020 to December 2021, 72 patients were included in the study who applied to the neurologic clinic because of symptoms compatible with carotid artery stenosis and had the carotid artery stenosis rate evaluated by Doppler ultrasound. The demographic variables of the participants were recorded (Table 1). The patients were divided into three groups as followings; Group 1 (mild stenosis): Patients with 29% or less stenosis; Group 2 (moderate stenosis): Patients with 30–70% stenosis; Group 3 (severe stenosis): Patients with 71-100% stenosis. Patients with no history of ocular conditions (except refractive errors myopia or hyperopia ± 2 D, astigmatism ± 1.5 D or presbyopia), healthy optic disc and an axial length inferior to 24 mm

were recruited. For each patient, only one eye was included in the study and if both eyes were eligible, then only one was randomly included in the study. Exclusion criteria included the following: history of chorioretinal or vitreoretinal diseases, glaucoma, history of intraocular surgery or trauma, best-corrected visual acuity of less than 20/25 or poor-quality image. In the study, controlled diabetes, arterial hypertension, hypercholesterolemia, and smoking status were also recorded to determine whether they have an influence on the choroid and retinal thickness.

Acquisition of OCT and OCTA Images

All participants underwent a comprehensive ophthalmic examination that consisted in best-corrected visual acuity using Snellen charts, intraocular pressure using a Goldman Applanation Tonometer, anterior segment slit-lamps biomicroscopy and funduscopic examinations using a 90 D lens after pupil mydriasis with 1% tropicamide solution.

The participants also underwent an optical coherence tomography and optical coherence tomography angiography with a Swept-source optical coherence tomography device (DRI OCT Triton plus, Topcon, Tokyo, Japan). Triton Swept-source optical coherence tomography operates at a 1050 nm wave-length that enables improved penetration into tissue with a A-scan rate of 100,000 per second and uses an innovative optical coherence tomography angiography algorithm, OCTARA (OCTA Ratio Analysis), that aims to provide improved detection sensitivity to low blood flow and reduced motion artifacts.[10] Thus, OCTARA is capable of visualizing the superficial retinal capillaries and foveal avascular zona, inner and outer retinal vascular plexuses, choriocapillaris, and larger choroidal vasculature in vivo without the need for contrast injection.

All measurements were performed by the same technician. The optical coherence tomography angiography images were obtained by the OCTARA algorithm. The macular 4.5 × 4.5-mm scan pattern centered at the fovea was used. Images were excluded from analyses if the image quality score was below 45 decibels (dB). Image quality scores were automatically generated by the software built into the OCT device. We used the boundaries for the superficial capillary plexus as automatically pre-set by the built-in software - from 2.6 µm beneath the internal limiting membrane to the 15.6 µm beneath the interface of the inner plexiform layer and inner nuclear layer (Fig. 1)-. Manually adjusted segmentation was required to obtain the rest of the capillary plexus following Method 3 described in Park et all[12] and based on Wang et al.[13] report: (1) middle capillary plexus from the 15.6 µm beneath the inner plexiform layer and inner nuclear layer to 31.2 µm beneath the inner plexiform layer and inner nuclear layer (Fig. 2); (2) deep capillary plexus from 31.2 µm beneath inner plexiform layer and inner nuclear layer to 70.2 µm beneath the inner plexiform layer and inner nuclear layer (Fig.3); (3) choriocapillaris from the Bruch membrane to 20 µm beneath the Bruch's membrane (Fig. 4);[14] (4) mid-choroid from 20 µm beneath the Bruch membrane to 56 µm beneath de Bruch membrane;[13] (5) deep choroid from 56 µm beneath the Bruch membrane to 100 µm beneath the Bruch membrane.

Vessel Density Calculation

The SS-OCTA software generates color-coded flow density maps and different vessel densities are then given numeric percentage values that reflect the percentage area occupied by blood density. Bright red color represents areas of highest density and dark blue represents areas of no detectable vessels. Intermediate colors represent variable grades of vessel density.[15,16] The vessel

density is automatically generated using the device's proprietary analysis tool. Capillary density values are obtained by applying an Early Treatment Diabetic Retinopathy Study grid overlay containing the two inner rings of the Early Treatment Diabetic Retinopathy Study grid pattern to fovea-centered OCTA images. Parafoveal retinal capillary densities from each of the four quadrants (superior, inferior, temporal and nasal) and from the ring centered to the fovea were used in subsequent analyses as well as a mean vessel density referred as global obtained by the average of the five and the paramacular retinal capillary density obtained by the average of the superior, inferior, temporal and nasal quadrants.

Statistical Analysis

The study data were analyzed in R-statistics 4.1.2 "Bird Hippie".[17] The sample size was calculated using the G Power 3.1.9.2 program, with the power of the research over 80%. Demographic and baseline characteristics were summarized as mean ± standard deviation for continuous variables and as percentages for categorical variables. Kolmogorov-Smirnov normality test was used for normality test. Unpaired student's t-test was used for the analysis of normally distributed binary groups, and ANOVA was used for the analysis of three groups. Mann–Whitney U-test was used in non-normally distributed binary groups, and Kruskal–Wallis H-test was used in the analysis of three groups. Bonferroni test adjustment was used when ANOVA or Kruskal-Wallis H-test were statistically significant. $P<0.05$ was accepted as statistically significant. Chi-squared and Fisher´s exact test analysis were performed to evaluate differences in the prevalence of the main risk factors for cardiovascular disease.

RESULTS

Demographics

A total of 72 eyes from 72 patients were included in the study. Group 1: 34 eyes (mean age: 70.8 ± 7.4); Group 2: 22 eyes (mean age: 70.4 ± 9.09); Group 3: 16 eyes (mean age: 75.27 ± 8.07). There were not significant differences in age, hypertension, diabetes mellitus, increase in cholesterol level and smoking among the three groups. The study demographics and clinical characteristics are summarized in Table 1.

Choriocapillaris Layer

Vessel density analysis in the choriocapillaris layer in patients with different degrees of carotid (Fig. 5) artery stenosis demonstrated no significant changes in any quadrant or in the global and paramacular regions. The vessel density data in the macula of the different study groups are summarized in Table 2.

Mid-choroid Layer

The vessel density values were significantly higher in patients with stenosis (group 2 and 3) compared with the control group (group 1), both in the paramacular region (P = .04) and the global value (P = .03) (Fig. 6). There were no significant differences between group 2 and 3.

The variance of the measurement by quadrants was higher than the paramacular and global measurements (Table 3).

Deep Choroid Layer

Similar to the mid-choroid plexus, deep choroid disclosed significantly superior vascular density values in group 3 compared to groups 2 and 1 in the paramacular area (P = .01) and globally (P = .04) (Fig. 7). There were no significant differences between group 1 and 2 (Table 4).

Superficial Capillary Plexus

There appeared to be a decrease in the vascular density values in group 3 compared to groups 1 and 2 (Fig. 8). However, no significant differences were detected in the paramacular region (P = .06) and with the global value (P = .12). The central quadrant increased in group 3 compared to 1 and 2, although the differences were not statistically significant (P = .38) (Table 5).

Mid-capillary Plexus

Vessel density analysis disclosed unremarkable differences among the three groups (Table 6) (Fig. 9).

Deep Capillary Plexus

The greater the degree of stenosis, the less vascular density values. However, these differences were not statistically significant in the paramacular area (P = .10) or globally (P = .44) (Fig. 10). The central quadrant, again, increased in group 3 compared to 1 and 2, although not significantly (P = .20) (Table 7).

DISCUSSION

Carotid artery stenosis is one of the principal causes of cerebral ischemic stroke, and its timely identification is of remarkable relevance for stroke prevention in the aging population. Generally, the prevalence of asymptomatic carotid artery stenosis in the overall population fluctuates between 1.6% to 5.7%.[4] A metanalysis displayed that the prevalence of ≥ 50% asymptomatic carotid artery stenosis oscillates between 0.2% in men < 50 years old and 7.5% in men aged ≥ 80 years. The prevalence of ≥ 70% asymptomatic carotid artery stenosis fluctuates between 0.1% in men aged < 50 years and 3.1% in ≥ 80 years old.[18] Delays in early identification and management could substantially aggravate patients' cognitive decline.

Clinical demonstrations of carotid artery stenosis, covering acute focal neurologic deficiencies, portray the hypoperfusion of the ipsilateral hemisphere. Frequently, the impaired structure is the internal carotid artery which plays a leading role in ocular perfusion as the ophthalmic artery directly arises from it. As a result of decreased eye perfusion, ocular alterations such as amaurosis fugax, retinal vascular occlusions and ocular ischemic syndrome may commonly occur. It is key to detect at risk population due to the potential irreversible nature of retinal damage.

As retinal and cerebral arterioles stem from a common germ layer, they share anatomical and physiological features.[19] Consequently, retinal microvascular anomalies are considered to be a reflection of the degree of cerebral microvascular affection.[20] Multiple previous studies suggest that ocular signs can mirror the alterations of carotid vessels, even the gravity of the stenosis.[21,22] Though, the capability of previously used examination methods is scarce as the invasive nature

of fluorescein angiography dissuades its application in asymptomatic patients[23] and other methodologies such as investigations on the retinal vascular using fundus images do not present sufficient precision for the monitoring of retinal microvascular plexuses in sufficient detail.[22] At the same time, the favorite examination technique for carotid artery stenosis in current practice is Duplex ultrasound, providing morphological features and allowing to quantify the magnitude of the stenosis. Although it is supposed to be a trustworthy diagnostic method when performed by a trained examiner, there are plenty human factors that could result in variability and error during ultrasound examinations.[24]

OCTA is a novel technology that offers high-resolution images of the macular region with high reliability and reproducibility. With the improvements of this new non-invasive modality, microvascular details in separate layers of the retina and choroid can be viewed quantitatively at the micrometer level, providing accurate data about the perfusion status of intraretinal capillaries.[10,25,26] OCTA has attracted an enormous amount of clinical research interest over the last years and is enlarging its daily use in clinical practice. Some reports have stated that patients with carotid artery stenosis present poor retinal microvasculature when compared with healthy controls.[27] Nevertheless, information on the correlation between the new retinal vascular metrics quantified by OCTA and carotid ultrasonographic parameters are largely lacking. In the current study, we conducted a quantitative review of macular capillary flow metered by vessel density, to investigate the correlation of OCTA-derived vascular metrics with carotid ultrasound stenosis rate.

To the best of our knowledge, our study is the first to document increased choroidal flow density in patients with higher degrees of carotid artery stenosis using SS-OCTA. Choroidal flow accounts for more than 85% of the ocular blood flow and, as foveal avascular zone has no retinal vascular supply, choroidal circulation plays a major role in this region.[28] However, to date, whether carotid artery stenosis influences the choroidal circulation is unknown. Reduced ocular blood flow may disturb vascular conformation and resistance, and further result in disruptions in the choroid following multiple compensation mechanisms such as collateral circulation (76% of the patients with carotid artery disease) or the presence of 'steal phenomenon' (26.8% of patients with more than 70% internal carotid artery stenosis). [29] Using the automatic quantification features of SS-OCTA, we objectively evaluated the choroidal vessel density and found that its measurements increase together with the degree of carotid artery stenosis. Previous OCTA publications did not find evidence any significant difference in the choriocapillaris before and after stenting in patients with carotid artery stenosis. [30] Similarly, our current report did not find a significant difference in the choriocapillaris between the three groups. Nevertheless, in Figure 4, a trend was noticeable in which mild or non-carotid artery stenosis patients appeared to have lower vessel density values than moderate and severe carotid artery stenosis patients. In the mid-choroid layer, mild stenosis presented significantly lower vessel density values compared to moderate and severe carotid artery stenosis and in the deep choroid layer, the severe carotid artery stenosis group presented with significantly higher vessel density values compared with mild and moderate carotid artery stenosis. This implies that the deeper the plexus is, the greater the degree of stenosis is necessary to induce an increase in vascular density.

The absence of agreement about the choroidal role in carotid artery stenosis could be justified considering the anastomotic organization of ocular vasculature. The complex structure of the choroid and deep anatomical location makes its study difficult using current OCTA devices, being SS-OCTA the most appropriate.[10] Because the primary role of the choroid is to nourish and thermoregulate the outer retina, an increase in vessel density might be a compensatory response that supplies more blood to an ischemic retina. A prominent issue to bear in mind is that collaterals through the ophthalmic artery may be recruited to compensate for reduced cerebral blood flow in patients with carotid artery stenosis. Nevertheless, although OCTA is fast, accurate and reproducible, presents a decisive limitation which is the absence of flow direction. To the best of our knowledge, this is the first study to examine the association between choroidal changes and different grades of carotid artery stenosis, although further studies should focus on the accurate analysis of the correlation between the amount of carotid artery stenosis and the alterations of the blood flow pressure of the posterior ciliary arteries.

There is proof that retinal capillary organization is an independent neurovascular unit at each capillary plexus where anomalies can occur independently.[31] Accordingly, some reports state that the retinal autoregulatory response to hyperoxia affects only the deep capillary plexus. In our study, patients with severe carotid artery stenosis presented a decreased flow density in the superficial and deep capillary plexuses when compared with non- carotid artery stenosis although these differences were not statistically significant. The relatively small sample size in every group may not have been sufficiently powered to detect a difference. This outcome is in line with previous studies that show worse retinal vascular parameters in subjects with carotid artery stenosis in the superficial capillary plexus but no significant differences in the deep capillary

plexus.[32] In contrast, other reports showed vessel density results disturbed only in the deep capillary plexus as it is considered to be primarily affected in several retinal conditions because of its lesser perfusion pressure and extremely fine morphology.[25] Consistently, a previous paper described that the maintenance of sufficient vessel density of deep capillary plexus was a protective factor of stroke. Nevertheless, the analysis of the deep retinal layer flow density values with OCTA should be cautiously interpreted since its quantification is affected by projection artefacts and the repeatability has been found to be weaker.[33] Thus, further investigations are needed on basis of the layer-related variations of the macular vascular density decrease.

At this point, it is worth noting that our results showed a standard deviation significantly lower in the paramacular region compared to the rest of the quadrants (superior, nasal, temporal and inferior) and the global vessel density in all the vascular layers. Thus, the paramacular vessel density value could have a higher discriminating power to detect the microvascular dysfunction caused by carotid artery stenosis when using OCTA ratio analysis (OCTARA).

Significantly, aside from carotid stenosis, the implications of other cardiovascular risk factors on the retinal microvasculature should not be ignored. The principal risk factors of carotid artery stenosis include smoking, obesity, age over 50 years, diabetes, hyperlipidemia, a cardiovascular event in a family member younger than 60 years, coronary disease, peripheral arterial disease, transient ischemic attack, or stroke.[34] When we chose patients in the three study groups, we matched their baseline data whereas the conditions in terms of hypertension, diabetes, smoking and hyperlipidemia. By this matching, we minimized the impact of non-carotid stenosis factors

on the results. However, large randomized controlled trial studies may be required to confirm the results.

We would like to acknowledge several limitations in our study. First, the study was performed using a relatively small number of patients. Further studies with a larger sample size are necessary to assess whether OCTA could be helpful as a potential biomarker in carotid artery stenosis. Second, abnormalities in retrobulbar hemodynamic metrics were not measured by Doppler ultrasonography. Documented retrobulbar blood flow insufficiency would imply more substantial effects on retinal microcirculation in patients with carotid artery stenosis. The observational design is another limitation; longitudinal studies are needed to validate our outcomes. Furthermore, our current study did not assess high-risk plaque features such as plaque length, echogenicity and/or surface area. Finally, since this is a cross-sectional study, it is not certain the duration of the stenosis, which could be an indicator for predicting a broad spectrum of neurological disorders.

Considering all the discoveries delivered by our investigation and previous studies, there is an overall accordance about the early implication of retinal blood flow perfusion, related with carotid artery stenosis, in asymptomatic patients. On the other hand, the contradictory outcomes might be associated with the limited number of included patients. However, to the best of our knowledge, our study is the first investigation to describe the relationship between microvascular features of the choroid and carotid artery stenosis parameters employing recently developed SS-OCTA quantitative approaches suggesting that imaging the retina and choroid via OCTA may be a promising tool to reflect the cerebral hemodynamic changes in carotid artery stenosis patients.

For these reasons, we believe our research was able to provide useful insights about the role of quantitative OCTA in detecting early retinal vascular alterations.

In conclusion, our current report provides the first evidence that choroidal microvascular changes were correlated with severity of carotid artery stenosis. Thus, OCTA can sensitively detect subtle changes in the ocular blood supply in the early stage of carotid artery stenosis representing a useful, fast, non-invasive, and objective approach to the retinal microvasculature. Therefore, this study may help establish a potential biomarker for predicting and monitoring hemodynamic changes in internal carotid artery stenosis. Future studies with larger sample size are needed to confirm our findings.

REFERENCES

1. Barnett HJ, Taylor DW, Eliasziw M, et al. Benefit of Carotid Endarterectomy in Patients with Symptomatic Moderate or Severe Stenosis. N Engl J Med 1998;339:1415-25.
2. Petty GW, Brown RD, Whisnant JP, et al. Ischemic Stroke Subtypes: a Population-Based Study of Incidence and Risk Factors. Stroke 1999;30:2513-6.
3. Feigin VL, Norrving B, George MG, et al. Prevention of Stroke: a Strategic Global Imperative. Nat Rev Neurol 2016;12:501-12.
4. de Weerd M, Greving JP, de Jong AW, et al. Prevalence of Asymptomatic Carotid Artery Stenosis According to Age and Sex: Systematic Review and Metaregression Analysis. Stroke 2009;40:1105-13.
5. Flaherty ML, Kissela B, Khoury JC, et al. Carotid Artery Stenosis as a Cause of Stroke. Neuroepidemiology 2013;40:36-41.
6. Montorsi P, Galli S, Ravagnani PM, Roffi M. Symptomatic Carotid Artery Disease: Revascularization. Prog Cardiovasc Dis 2017;59:601-11.
7. Cohen R, Padilla J, Light D, Diller R. Carotid Artery Occlusive Disease and Ocular Manifestations: Importance of Identifying Patients at Risk. Optometry 2010;81:359-63.
8. De Silva DA, Manzano JJ, Liu EY, et al. Retinal Microvascular Changes and Subsequent Vascular Events After Ischemic Stroke. Neurology 2011;77:896-903.
9. Seidelmann SB, Claggett B, Bravo PE, et al. Retinal Vessel Calibers in Predicting Long-Term Cardiovascular Outcomes: The Atherosclerosis Risk in Communities Study. Circulation 2016;134:1328-38.
10. Stanga PE, Tsamis E, Papayannis A, et al. Swept-Source Optical Coherence Tomography Angio^{TM} (Topcon Corp, Japan): Technology Review. Dev Ophthalmol 2016;56:13-7.

11. Miller AR, Roisman L, Zhang Q, et al. Comparison Between Spectral-Domain and Swept-Source Optical Coherence Tomography Angiographic Imaging of Choroidal Neovascularization. Invest Ophthalmol Vis Sci 2017;58:1499-505.
12. Park JJ, Soetikno BT, Fawzi AA. Characterization of the Middle Capillary Plexus Using Optical Coherence Tomography Angiography in Healthy and Diabetic Eyes. Retina Phila Pa 2016;36:2039-50.
13. Wang E, Zhao X, Yang J, Chen Y. Visualization of Deep Choroidal Vasculatures and Measurement of Choroidal Vascular Density: A Swept-source Optical Coherence Tomography Angiography Approach. BMC Ophthalmol 2020;20:321.
14. Chu Z, Zhang Q, Gregori G, et al. Guidelines for Imaging the Choriocapillaris Using OCT Angiography. Am J Ophthalmol 2021;222:92-101.
15. Sambhav K, Grover S, Chalam KV. The Application of Optical Coherence Tomography Angiography in Retinal Diseases. Surv Ophthalmol 2017;62:838-66.
16. Moussa M, Leila M, Bessa AS, et al. Grading of Macular Perfusion in Retinal Vein Occlusion Using En-Face Swept-Source Optical Coherence Tomography Angiography: A Retrospective Observational Case Series. BMC Ophthalmol 2019;19:127.
17. R Core Team. R: A Language And Environment For Statistical Computing. Vienna R Foundation for Statistical Computing; 2019. Available at: https://www.R-project.org. Accessed September 7, 2023.
18. de Weerd M, Greving JP, Hedblad B, et al. Prevalence of Asymptomatic Carotid Artery Stenosis in the General Population: an Individual Participant Data Meta-Analysis. Stroke 2010;41:1294-7.

19. Toma N. Anatomy of the Ophthalmic Artery: Embryological Consideration. Neurol Med Chir (Tokyo) 2016;56:585-91.

20. Wong TY, Klein R, Couper DJ, et al. Retinal Microvascular Abnormalities And Incident Stroke: The Atherosclerosis Risk in Communities Study. Lancet 2001;358:1134-40.

21. Lareyre F, Nguyen E, Raffort J, et al. Changes in Ocular Subfoveal Choroidal Thickness After Carotid Endarterectomy Using Enhanced Depth Imaging Optical Coherence Tomography: A Pilot Study. Angiology 2018;69:574-81.

22. Machalińska A, Kawa MP, Babiak K, et al. Retinal Vessel Dynamic Functionality in the Eyes of Asymptomatic Patients with Significant Internal Carotid Artery Stenosis. Int Angiol 2019;38:230-8.

23. Wang J, Wang W, Jin B, et al. Improvement in Cerebral and Ocular Hemodynamics Early after Carotid Endarterectomy in Patients of Severe Carotid Artery Stenosis with or without Contralateral Carotid Occlusion. BioMed Res Int 2016;2016:2901028.

24. Lui EYL, Steinman AH, Cobbold RS, Johnston KW. Human Factors as a Source of Error in Peak Doppler Velocity Measurement. J Vasc Surg 2005;42:972-9.

25. Arrigo A, Corbelli E, Aragona E, et al. Optical Coherence Tomography and Optical Coherence Tomography Angiography Evaluation Of Combined Hamartoma of the Retina and Retinal Pigment Epithelium. Retina Phila Pa 2019;39:1009-15.

26. de Carlo TE, Romano A, Waheed NK, Duker JS. A Review of Optical Coherence Tomography Angiography (OCTA). Int J Retina Vitr 2015;1:5.

27. Sayin N, Kara N, Uzun F, et al. A Quantitative Evaluation of the Posterior Segment of the Eye Using Spectral-Domain Optical Coherence Tomography in Carotid Artery Stenosis: A Pilot Study. Ophthalmic Surg Lasers Imaging Retina 2015;46:180-5.

28. Nickla DL, Wallman J. The Multifunctional Choroid. Prog Retin Eye Res 2010;29:144-68.
29. Costa VP, Kuzniec S, Molnar LJ, et al. Collateral Blood Supply through the Ophthalmic Artery: A Steal Phenomenon Analyzed by Color Doppler Imaging. Ophthalmol 1998;105:689-93.
30. Li XY, Zhu SY, Zhou SJ, et al. Optical Coherence Tomography Angiography as a Noninvasive Assessment of Cerebral Microcirculatory Disorders Caused by Carotid Artery Stenosis. Dis Markers 2021;2021:2662031.
31. Hagag AM, Pechauer AD, Liu L, et al. OCT Angiography Changes in the 3 Parafoveal Retinal Plexuses in Response to Hyperoxia. Ophthalmol Retina 2018;2:329-36.
32. Lahme L, Marchiori E, Panuccio G, et al. Changes in Retinal Flow Density Measured by Optical Coherence Tomography Angiography in Patients with Carotid Artery Stenosis after Carotid Endarterectomy. Sci Rep 2018;8:17161.
33. Spaide RF, Fujimoto JG, Waheed NK. Image Artifacts in Optical Coherence Tomography Angiography. Retina-J Ret Vit Dis 2015;35:2163-80.
34. Mathiesen EB, Joakimsen O, Bønaa KH. Prevalence of and Risk Factors Associated with Carotid Artery Stenosis: The Tromsø Study. Cerebrovasc Dis Basel Switz 2001;12:44-51.

Table 1. Characteristics of participants. Groups 1: mild stenosis group; group 2: moderate stenosis; group 3: severe stenosis.

	Group 1 (n=34)	Group 2 (n=22)	Group 3 (n=16)	*P*
Gender, male (%)	41.1	54.5%	62.5%	> .05
Age, years	70.8	70.4	75.2	> .05
Hypertension (%)	76.5	90.9	90.9	> .05
Diabetes (%)	47.1	45.5	54.5	> .05
Hyperlipidaemia (%)	91.2	86.4	100.0	> .05
Current smoker (%)	44.1	54.5	54.5	> .05

Table 2. Mean vessel density (%) per quadrant in choriocapillaris. Groups 1: mild stenosis group; group 2: moderate stenosis; group 3: severe stenosis. (ZAF = Foveal Avascular Zone)

	Group 1 (n=34)	Group 2 (n=22)	Group 3 (n=16)
Global	52.38 ± 2.22	53.05 ± 2.05	52.73 ± 1.27
Paramacular	52.68 ± 2.70	53.56 ± 2.00	53.48 ± 1.02
Inferior	53.06 ± 3.08	54.85 ± 3.53	54.25 ± 1.45
Nasal	53.00 ± 3.24	53.10 ± 3.72	52.84 ± 2.03
Superior	51.95 ± 3.36	52.26 ± 4.06	52.68 ± 3.04
Temporal	52.70 ± 8.75	54.02 ± 3.65	54.14 ± 2.77
ZAF	50.32 ± 5.52	50.95 ± 6.54	49.76 ± 4.63

Table 3. Mean vessel density (%) per quadrant in mid choroid. *Statistically significant differences between the groups. Groups 1: mild stenosis group; group 2: moderate stenosis; group 3: severe stenosis (ZAF = Foveal Avascular Zone)

	Group 1 (n=34)	Group 2 (n=22)	Group 3 (n=16)
Global	52.92 ± 1.85	53.93 ± 2.24	53.93 ± 1.43 *
Paramacular	52.54 ± 2.11	53.51 ± 2.54	53.84 ± 1.12 *
Inferior	52.91 ± 4.10	54.91 ± 4.38	54.89 ± 3.01
Nasal	52.14 ± 4.29	54.25 ± 4.55	53.87 ± 2.47
Superior	50.99 ± 4.98	51.29 ± 5.14	52.44 ± 2.53
Temporal	54.11 ± 3.88	53.59 ± 4.25	54.16 ± 2.77
ZAF	54.48 ± 6.45	55.63 ± 7.98	54.30 ± 5.92

Table 4. Mean vessel density (%) per quadrant in deep choroid. *Statistically significant differences between the groups. Groups 1: mild stenosis group; group 2: moderate stenosis; group 3: severe stenosis (ZAF = Foveal Avascular Zone).

	Group 1 (n=34)	Group 2 (n=22)	Group 3 (n=16)
Global	46.32 ± 3.21	47.03 ± 3.10	49.19 ± 2.61 *
Paramacular	45.53 ± 3.30	45.77 ± 3.48	49.11 ± 3.07 *
Inferior	45.75 ± 7.72	46.48 ± 6.54	52.71 ± 4.70
Nasal	45.00 ± 6.23	45.53 ± 4.68	49.58 ± 7.07
Superior	44.27 ± 6.40	43.60 ± 7.11	46.18 ± 4.03
Temporal	47.08 ± 5.33	47.46 ± 5.80	47.96 ± 2.87
ZAF	49.48 ± 7.61	52.10 ± 9.49	49.51 ± 9.46

Table 5. Mean vessel density (%) per quadrant in superficial capillary plexus. Groups 1: mild stenosis group; group 2: moderate stenosis; group 3: severe stenosis (ZAF = Foveal Avascular Zone).

	Group 1 (n=34)	Group 2 (n=22)	Group 3 (n=16)
Global	39.35 ± 2.24	39.68 ± 2.14	38.18 ± 2.35
Paramacular	45.64 ± 2.59	46.07 ± 2.78	43.72 ± 3.10
Inferior	47.82 ± 4.03	48.01 ± 5.04	45.06 ± 4.34
Nasal	42.73 ± 3.97	42.78 ± 3.27	42.02 ± 4.01
Superior	47.32 ± 3.66	47.69 ± 3.72	44.50 ± 4.46
Temporal	44.69 ± 3.13	45.81 ± 2.93	43.30 ± 5.26
ZAF	14.20 ± 3.77	14.10 ± 3.46	16.01 ± 6.20

Table 6. Mean vessel density (%) per quadrant in middle capillary plexus. Groups 1: mild stenosis group; group 2: moderate stenosis; group 3: severe stenosis (ZAF = Foveal Avascular Zone).

	Group 1 (n=34)	Group 2 (n=22)	Group 3 (n=16)
Global	39.31 ± 2.40	39.44 ± 1.62	39.16 ± 2.69
Paramacular	43.67 ± 2.99	43.50 ± 2.80	43.23 ± 2.76
Inferior	44.31 ± 6.00	44.00 ± 4.56	42.85 ± 4.61
Nasal	42.48 ± 5.51	42.34 ± 4.17	43.89 ± 4.35
Superior	43.75 ± 4.65	43.48 ± 3.72	41.98 ± 6.18
Temporal	44.14 ± 4.09	44.18 ± 3.93	44.22 ± 5.79
ZAF	21.89 ± 8.07	23.19 ± 7.52	22.87 ± 9.06

Table 7. Mean vessel density (%) per quadrant in deep capillary plexus. Groups 1: mild stenosis group; group 2: moderate stenosis; group 3: severe stenosis (ZAF = Foveal Avascular Zone).

	Group 1 (n=34)	Group 2 (n=22)	Group 3 (n=16)
Global	42.22 ± 1.96	42.01 ± 2.25	41.41 ± 3.02
Paramacular	46.39 ± 0.04	46.42 ± 0.18	46.39 ± 0.01
Inferior	52.06 ± 4.24	51.59 ± 5.05	51.28 ± 3.66
Nasal	47.75 ± 4.38	46.35 ± 5.51	46.67 ± 5.34
Superior	53.03 ± 4.37	51.78 ± 3.61	49.24 ± 4.79
Temporal	47.18 ± 4.04	48.61 ± 3.69	45.36 ± 6.99
ZAF	11.09 ± 5.02	11.70 ± 5.20	14.50 ± 7.20

FIGURE LEGENDS

Figure 1.- Example of a 4,5 x 4,5 mm macular color-coded flow density map and vessel density map showing the foveal and parafoveal subfields (superior, temporal inferior, and nasal) automatically segmented in the superficial capillary plexus.

Figure 2.- Example of a 4,5 x 4,5 mm macular color-coded flow density map and vessel density map showing the foveal and parafoveal subfields (superior, temporal inferior, and nasal) manually segmented in the middle capillary plexus.

Figure 3.- Example of a 4,5 x 4,5 mm macular color-coded flow density map and vessel density map showing the foveal and parafoveal subfields (superior, temporal inferior, and nasal) manually segmented in the middle capillary plexus.

Figure 4.- Example of a 4,5 x 4,5 mm macular color-coded flow density map and vessel density map showing the foveal and parafoveal subfields (superior, temporal inferior, and nasal) manually segmented in the choriocapillaris.

Figure 5. Choriocapillaris layer. Distribution of mean vessel density in the different quadrants measured. G = global region; I = inferior quadrant; N = nasal quadrant; P = paramacular region; S = superior quadrant; T = temporal quadrant; ZAF = foveal avascular zone.

Figure 6. Mid-choroid layer. **(A)** Distribution of mean vessel density in the different quadrants measured. G = global region; I = inferior quadrant; N = nasal quadrant; P = paramacular region; S = superior quadrant; T = temporal quadrant; ZAF = foveal avascular zone. **(B)** Box and whisker plot showing the differences between group 1 and Group 2 in the paramacular area and **(C)** in the global region.

Figure 7. Deep choroid layer. **(A)** Distribution of mean vessel density in the different quadrants measured. G = global region; I = inferior quadrant; N = nasal quadrant; P = paramacular

region; S = superior quadrant; T = temporal quadrant; ZAF = foveal avascular zone. B) Box and whisker plot showing the differences between group 1 and Group 2 in the paramacular area and **(C)** in the global region.

Figure 8. Superficial capillary plexus. **(A)** Distribution of mean vessel density in the different quadrants measured. G = global region; I = inferior quadrant; N = nasal quadrant; P = paramacular region; S = superior quadrant; T = temporal quadrant; ZAF = foveal avascular zone. **(B)** Box and whisker plot showing the differences between group 1 and Group 2 in the paramacular area and **(C)** in the global region. **(D)** Plot of means showing the mean vessel density in the foveal avascular zona quadrant in the different groups.

Figure 9. Mid-capillary plexus. Distribution of mean vessel density in the different quadrants measured. G = global region; I = inferior quadrant; N = nasal quadrant; P = paramacular region; S = superior quadrant; T = temporal quadrant.

Figure 10. Deep capillary plexus. **(A)** Distribution of mean vessel density in the different quadrants measured. G = global region; I = inferior quadrant; N = nasal quadrant; P = paramacular region; S = superior quadrant; T = temporal quadrant; ZAF = foveal avascular zone. **(B)** Box and whisker plot showing the differences between group 1 and Group 2 in the paramacular area and **(C)** in the global region. **(D)** Plot of means showing the mean vessel density in the foveal avascular zona quadrant in the different groups.

Figure 1

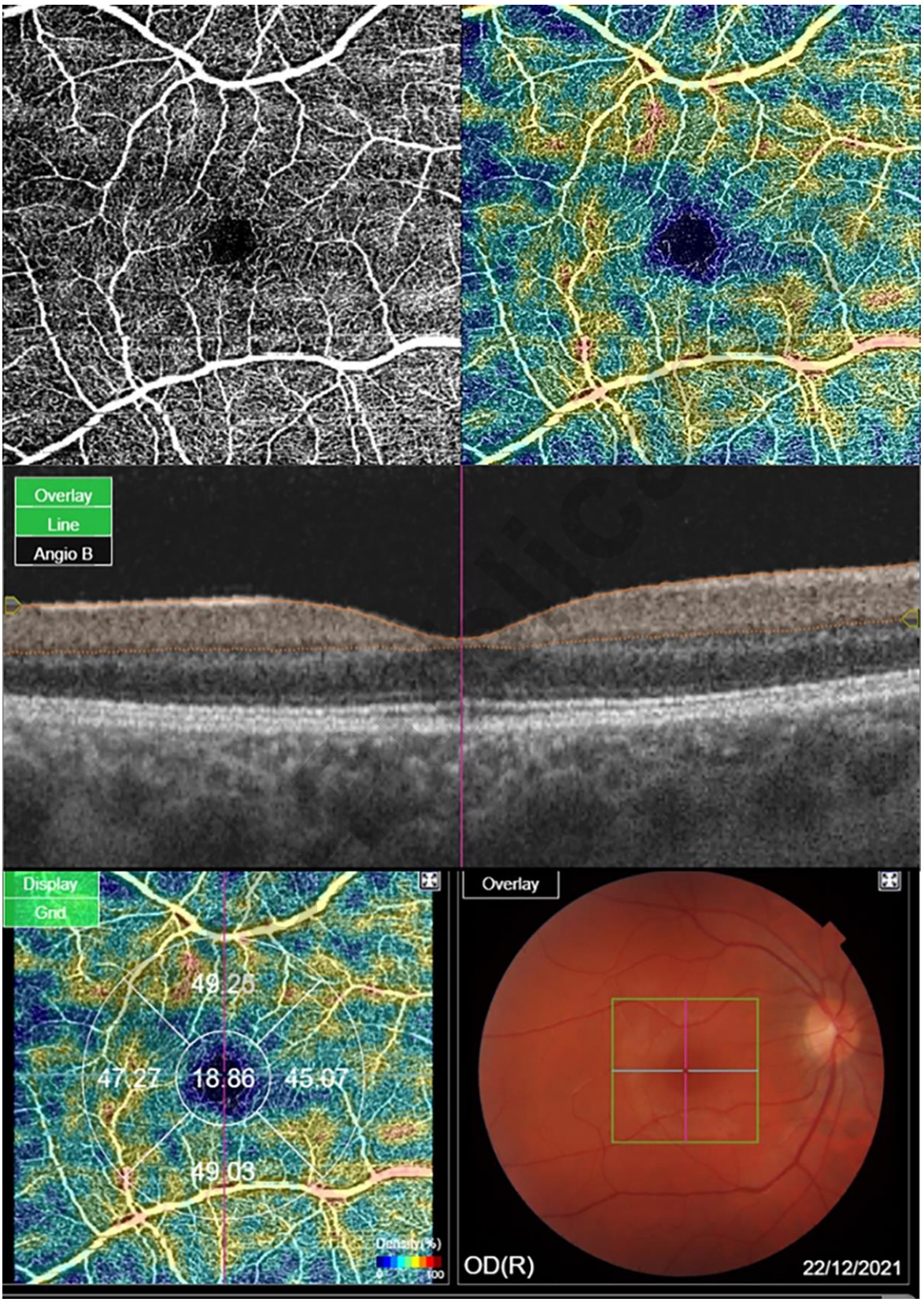

Figure 2

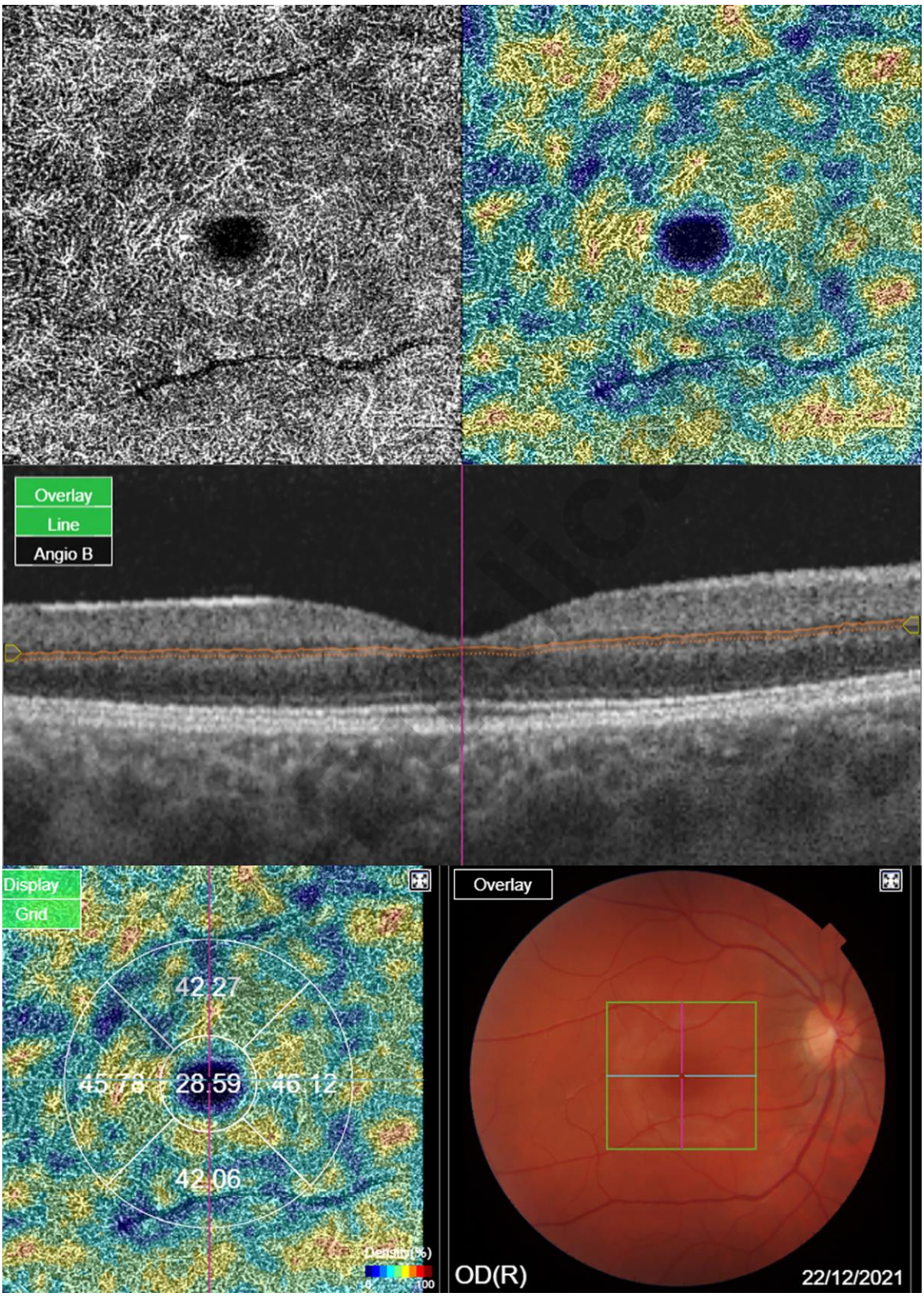

Figure 3

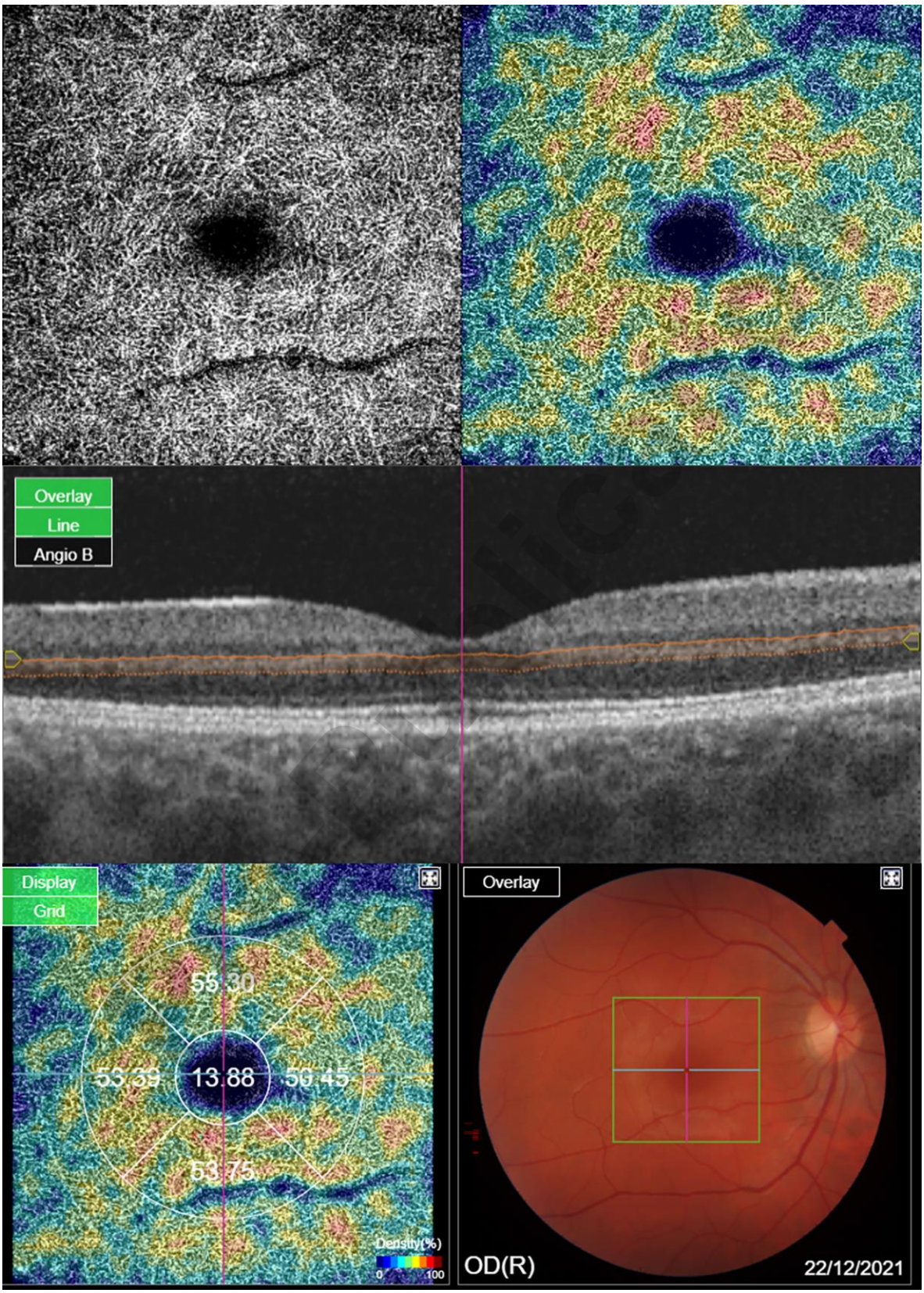

Figure 4

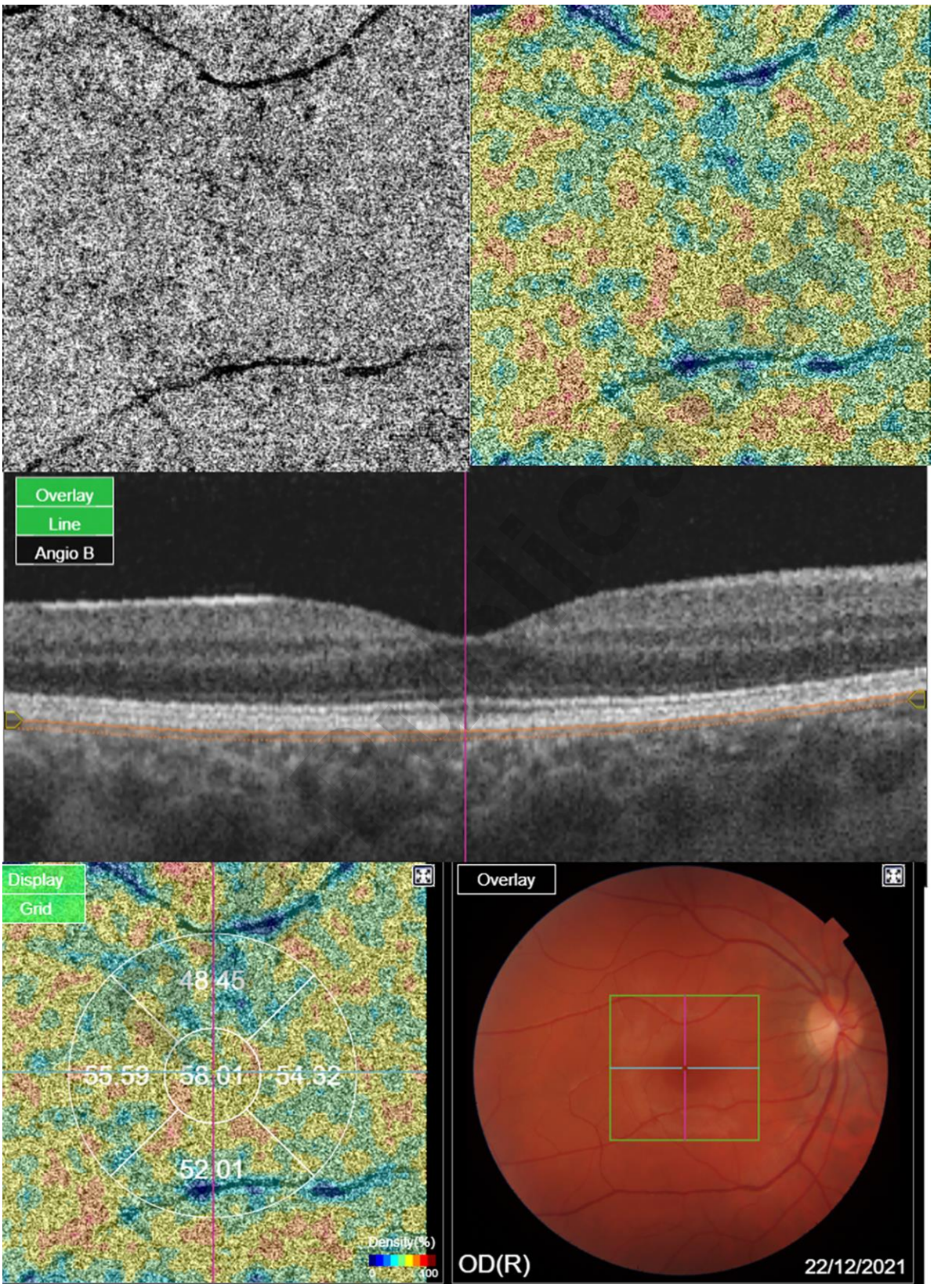

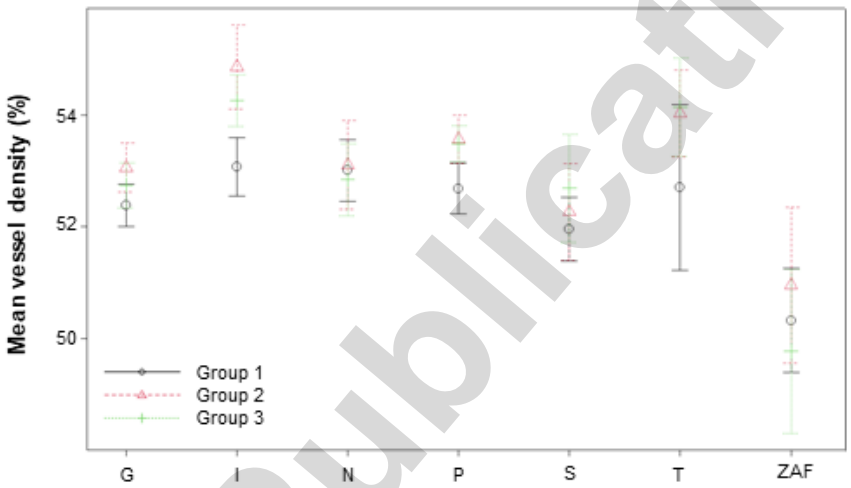

Figure 5 reformattedKAZ

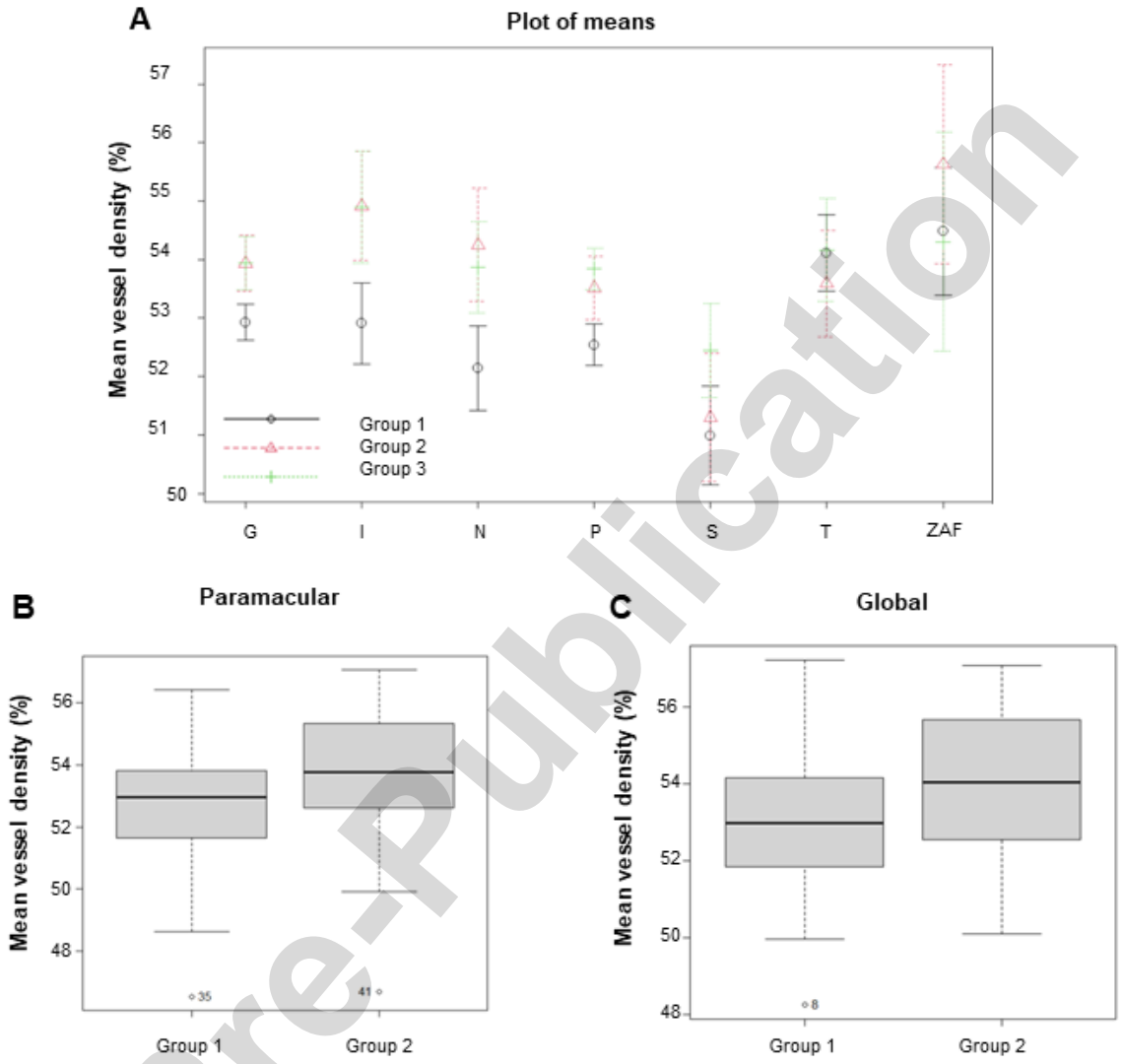

Figure 6 reformattedKAZ

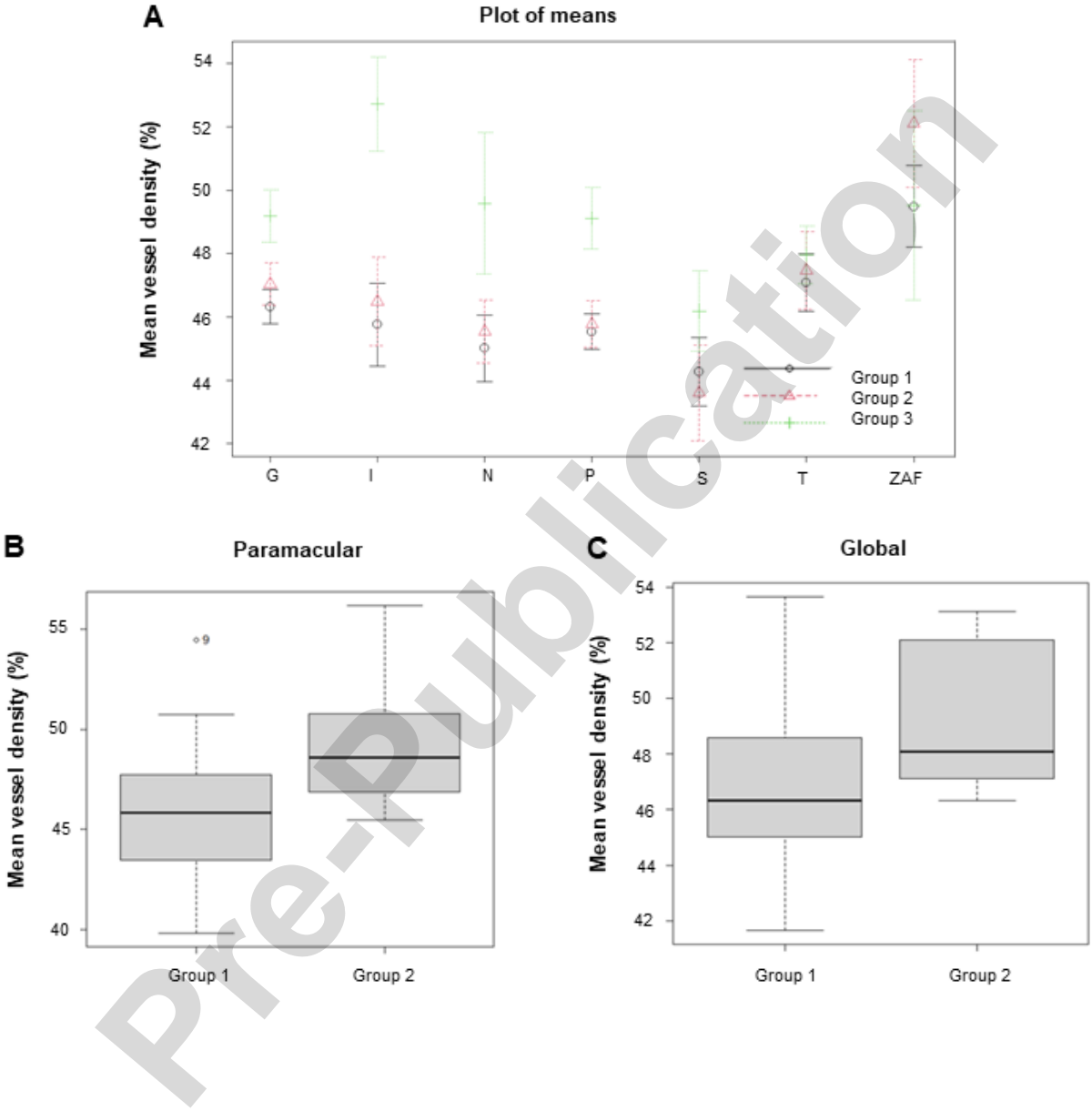

Figure 7 reformattedKAZ

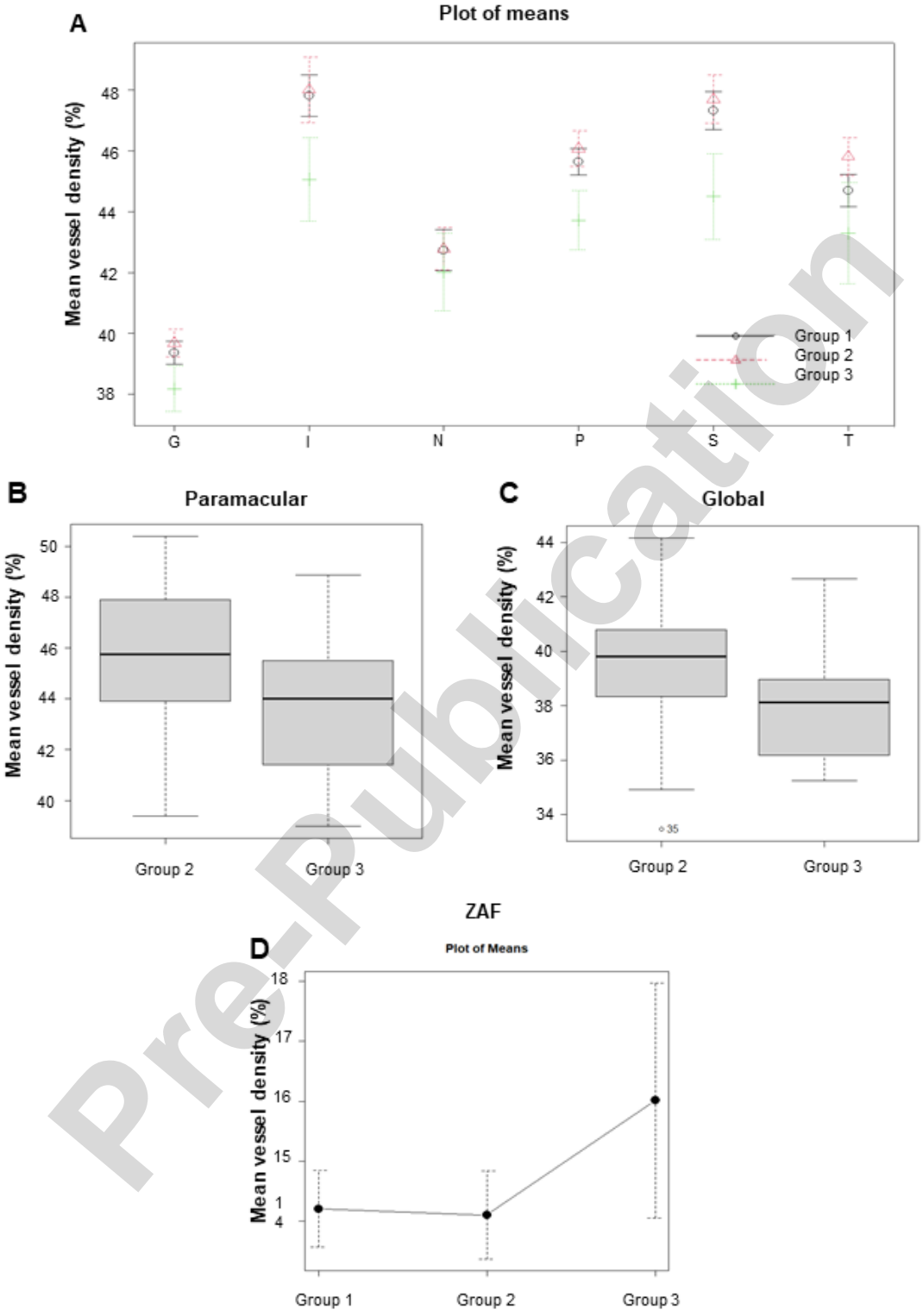

Figure 8 reformattedKAZ

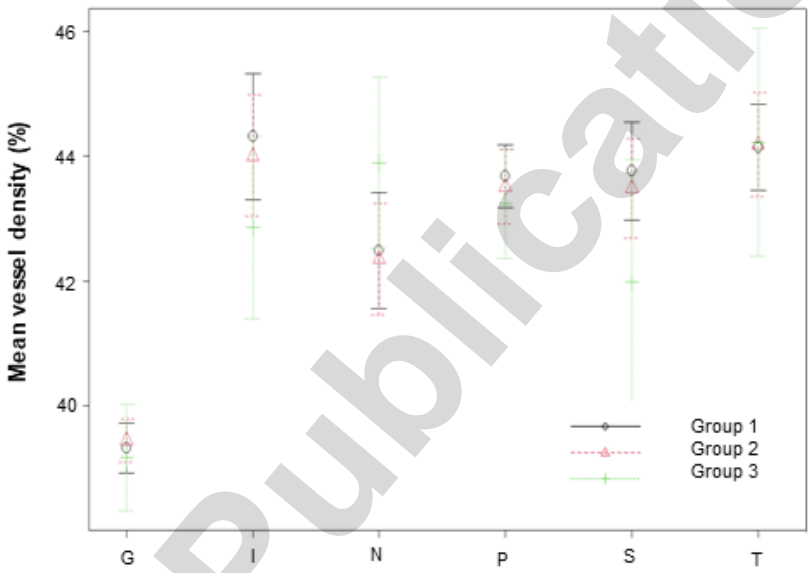

Figure 9 reformattedKAZ

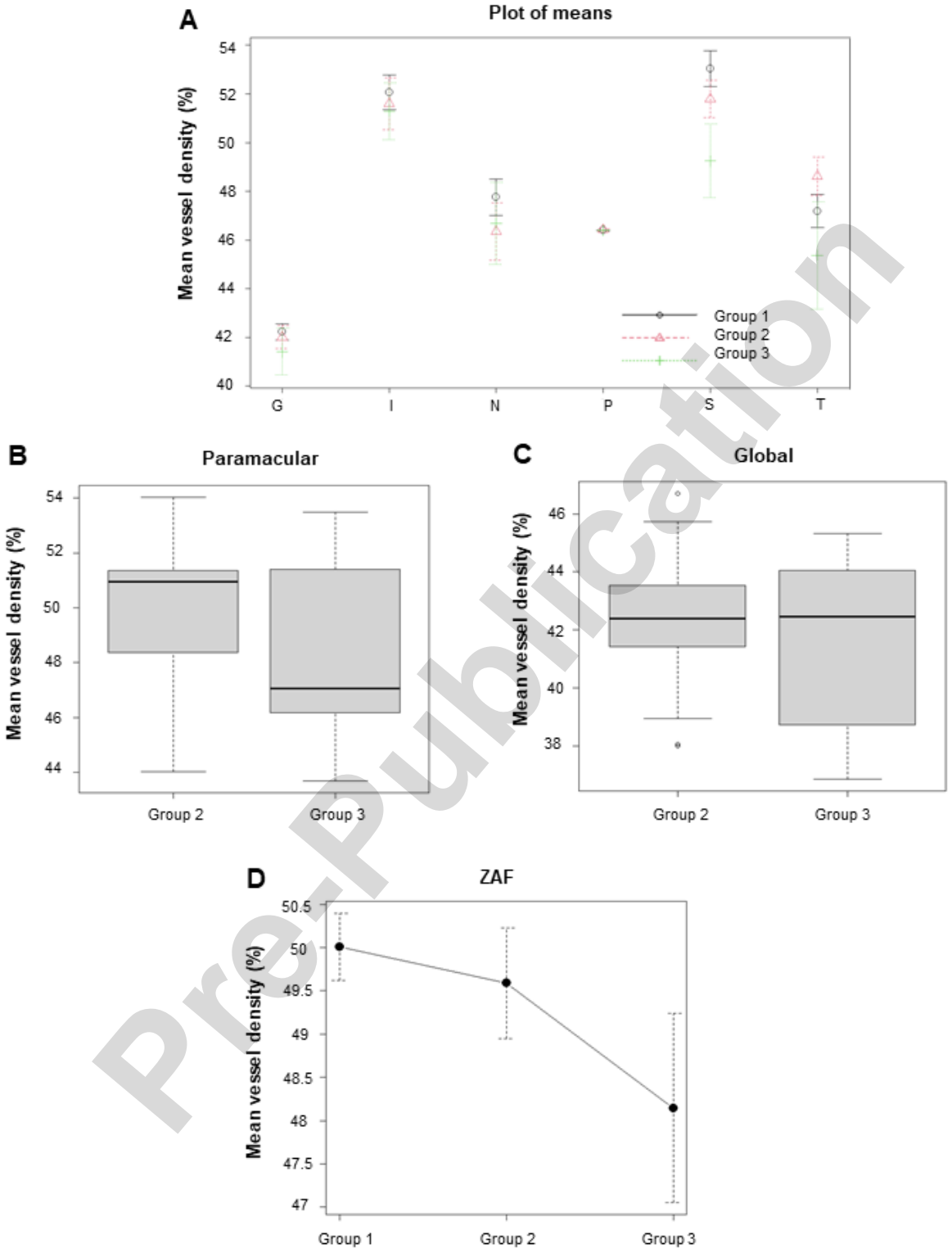

Figure 10 reformattedKAZ